Journal of Photochemistry and Photobiology A: Chemistry 207 (2009) 181–189

Contents lists available at ScienceDirect

Journal of Photochemistry and Photobiology A: Chemistry

journal homepage: www.elsevier.com/locate/jphotochem

A pair of regio-isomeric compounds acting as molecular logic gates with different functions

Junhong Qian, Yufang Xu, Xuhong Qian*, Shenyi Zhang

Shanghai Key Laboratory of Chemical Biology, School of Pharmacy, East China University of Science and Technology, Shanghai 200237, PR China

ARTICLE INFO

Article history:
Received 3 March 2009
Received in revised form 6 June 2009
Accepted 3 July 2009
Available online 3 August 2009

Keywords:
Molecular logic gate
Isomer
Surfactant
pH

ABSTRACT

Regioisomers **6a** and **6b** display different spectral properties towards pH and surfactant concentration. For compound **6a**, an obvious color change from yellow to red and significant fluorescence quenching were observed upon addition of acid, whereas large enhancements in emission and absorption intensities of **6b** were found with decreasing pH value. CTAB and Triton X-100 enhanced the fluorescence intensity of both dyes. Small amount of SDS (less than its cmc) quenched, while large amount of SDS ([SDS] > cmc) recovered the fluorescence of **6a** and **6b**. **6a** and **6b** can execute different Boolean operations: much more logic functions can be implemented with **6a** in SDS system, while half addition can be realized with **6b** when both inputs are SDS.

1. Introduction

The molecular logic gates emerged with the development of fluorescent molecular sensors, which set up a bridge between information technology and chemistry [1–8]. Molecular computation is a long-term goal, but the progress in molecular-scale information processing will simulate the advances of this goal. Many researchers have paid much attention to the design of molecular devices for performing Boolean operation during the past two decades [9–24]. However, restricted by fewer types of configurable logic functions, molecular calculations are relatively limited. So, construction of molecular systems with multiple logic functions is of particular interest [25–30].

Surfactants, with versatility related to their concentrations, have been used in many scientific researches. For instance, surfactant aggregates have been cleverly used for the self-assembled nanoreactors [31] or for the template synthesis of novel mesoporous materials [32] because of their container properties; surfactant micelles can modulate the sensitivity of ion determination due to the amplifying effect on the local ion concentration [33–37]; they can also be exploited for mimicking biological membrane based on the membrane-similar microenvironment properties provided by different surfactant assembles [38–40], etc. If a tailor-made small fluorescent sensor molecule could share the virtues that surfactant provides, and then large-amplitude performance elevation may be realized, which may open a possible way to construct supramolecular systems for behaving as molecular logic gates [41–43]. As a consequence, more logic functions as well as logic calculations might be performed at molecular level in surfactant systems [44,45]. We have systemically studied the effects of different kinds of surfactants on the photophysical properties of the two regio-isomeric compounds **6a** and **6b** as well as different molecular logic functions executed by them in SDS aqueous solution. The results showed that: (1) **6a** and **6b** are "off–on–off" and "on–off" fluorescent pH sensors, respectively; (2) both **6a** and **6b** are sensitive to the microenvironmental polarity; (3) in CTAB and Triton X-100 micellar systems, the fluorescence intensities of **6a** and **6b** were enhanced, while those of the compounds shown in our previous work had no obvious change [44,45]; (4) different from the results reported in our previous work [44], regioisomers **6a** and **6b** implement different logic functions with the assistance of SDS: **6a** can execute more logic functions, while **6b** can realize logic calculation.

2. Experimental

2.1. Reagents

All the solvents and reagents were of analytic grade and used as received, sodium dodecylsulfate (SDS, Sigma, 99%), cetyltrimethylammonium bromide (CTAB, Sigma), Triton X-100 (Sigma), water used was twice distilled.

2.2. Absorbance and fluorescence titration

In pH titration experiments, the pH values were adjusted with 5 M NaOH and HCl aqueous solution. The pH was determined with a

* Corresponding author.
E-mail address: xhqian@ecust.edu.cn (X. Qian).

1010-6030/$ – see front matter © 2009 Elsevier B.V. All rights reserved.
doi:10.1016/j.jphotochem.2009.07.006

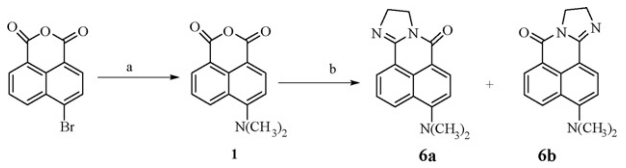

Scheme 1. Preparation of **6a** and **6b**. Reagents: (a) 37% $NH(CH_3)_2$ aqueous solution, DMF, $CuSO_4$ (b) $NH_2C_2H_4NH_2$, $CH_3OC_2H_4OH$.

pH meter (Shanghai Rex Instrument Factory, China; model PHS-3C), which was standardized with Aldrich buffers. Absorption measurements were performed with a Varian Cary 500 spectrophotometer (1 cm quartz cell) and fluorescence spectra were recorded on a Varian Cary Eclipse fluorescence spectrophotometer (1 cm quartz cell). Mass spectra (MS) were recorded on an MA1212 instrument using standard conditions (ESI, 70 eV). All the experiments were performed at 25.0 ± 0.1 °C. In surfactant titration experiments, no control was made on the pH, which was the natural value for each solution (pH = 6.50 ± 0.10 in micellar systems).

2.3. Synthesis

The synthesis of isomers dihydroimidazo [2,1-*a*] [6′-(N,N-dimethyl)-amino] benz [*de*] isoquinolin-7-one **(6a)** and 3-(N,N-dimethyl)-amino dihydroimidazo [2,1-*a*] benz [*de*] isoquinolin-7-one **(6b)** from commercially available compounds is illustrated in Scheme 1.

2.3.1. 4-N,N-(dimethyl) aminonaphthalene-1,8-dicarboximide (*1*)

2.0 mL of dimethylamine aqueous solution and catalytic amount of $CuSO_4$ were added to a suspension of 4-bromonaphthalene-1,8-dicarboximide (5.54 g, 2 mmol) in DMF (50 mL). The mixture was then refluxed for 1.5 h, after which the solvent was evaporated under vacuum. The product **1** was crystallized from ethanol. Yield: 90%. M.p. 134.8 °C; MS: m/z (%) 241 (1%); ^{1}H NMR (500 MHz, $CDCl_3$): δ 8.57 (dd, 1H), 8.55 (dd, 1H), 8.47 (d, *J* = 8.3 Hz, 1H), 7.66 (t, *J* = 7.6 Hz, 1H), 7.11 (d, *J* = 8.3 Hz, 1H), 3.13 (s, 6H).

2.3.2. *6a* and *6b*

To a solution of 5 mL of ethylene glycol monomethyl ether added 0.2 g (6.3 mmol) of **1** and excess ethylenediamine (1 mL). The mixture was refluxed for 5 h under N_2 atmosphere and then the solvent was evaporated under vacuum. The product was purified by chromatography using methanol/dichloromethane (1:50, v/v) as eluant to give 40 mg (20%) of **6a** as orange red solid: ^{1}H NMR (CDCl3): δ 8.50 (d, *J* = 7.5 Hz, 1H), 8.36 (d, *J* = 8.2 Hz, 2H), 7.62 (t, *J* = 7.5 Hz, 1H), 7.11 (d, *J* = 7.9 Hz, 1H), 4.23 (t, 2H), 4.18 (t, 2H), 3.05 (s, 6H). HR-MS (ES+) Calcd. for ([M+H])$^+$, 266.1293; Found: 266.1289. **6b** was obtained by the same procedure as orange solid (yield 45%): ^{1}H NMR (CDCl3): δ 8.65 (s, 1H), 8.51–8.32 (d, 2H), 7.65 (s, 1H), 7.16 (s, 1H), 4.22 (s, 4H), 3.12 (s, 6H). HR-MS (ES+) Calcd. for ([M+H])$^+$, 266.1293; Found: 266.1286.

3. Principles

Regioisomers **6a** and **6b** were designed as fluorescent ICT pH sensors. In **6a** and **6b**, the fluorophore is a strong "push–pull" π-electron system, with the N,N-dimethylamino group as the electron donor, and two electron-deficient groups, carbonyl and H^+ receptor imine (C=N) in dihydroimidazole heterocycle, as the electron acceptors. When the imine nitrogen catches a H^+ ion, π-electron conjugation within the fluorophore will be significantly perturbed and the spectral properties will be affected to a large extent (such as wavelength shifts, changes in fluorescence intensity and absorbance) [46–48]. In addition, the 4 (or 5)-substituting N,N-dimethylamino group induces another excited state, namely TICT (twisted intramolecular charge transfer) state, which is affected by the polarity of solvent. So, the photophysical properties of **6a** and **6b** vary with solvents.

Scheme 2 shows that the imine in **6a** and **6b** can be protonated at higher H^+ concentrations, which makes the ICT process more efficient and will cause a considerable bathochromic shift in absorption band. But it opens up non-radiative deexcitation pathways, such as the solvation of water [49], and quenches the fluorescence. At higher OH^- concentrations, the naphthalene-1,8-dicarboximide cycle will be decyclized, and the fluorescence quenching is caused by the molecular vibration.

4. Results and discussions

4.1. pH effect on the spectral properties of isomers *6a* and *6b*

The absorption and emission spectra of **6a** and **6b** are strongly dependent on the pH, but they display remarkably different spectral response towards pH. Addition of hydrochloric acid to **6a** in alkaline aqueous solution showed a color change which was perceptible to the naked eye, from yellow to red. The decrease of pH led to ~102 nm red-shift in the absorption maximum: a significant decrease in 398 nm and increase in a new longer absorption band (500 nm, Fig. 1a), and an isosbestic point at 445 nm was clearly observed.

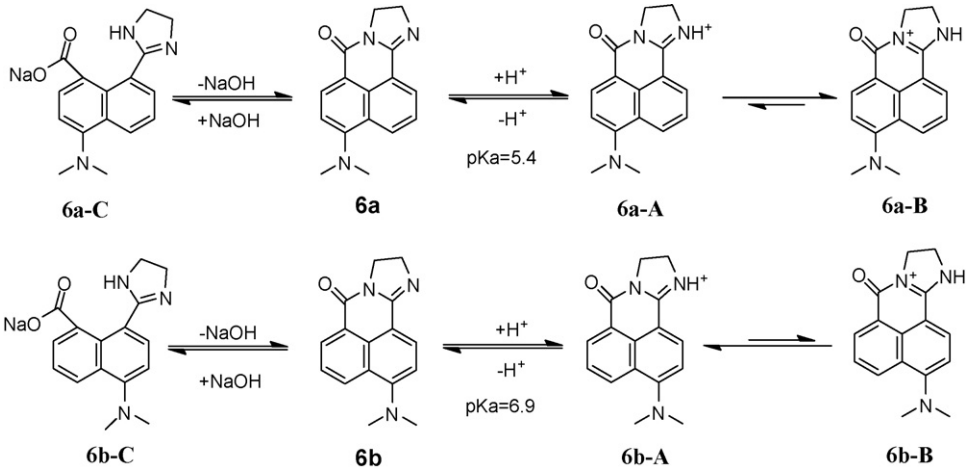

Scheme 2. The protonation and decyclization processes of **6a** and **6b**.

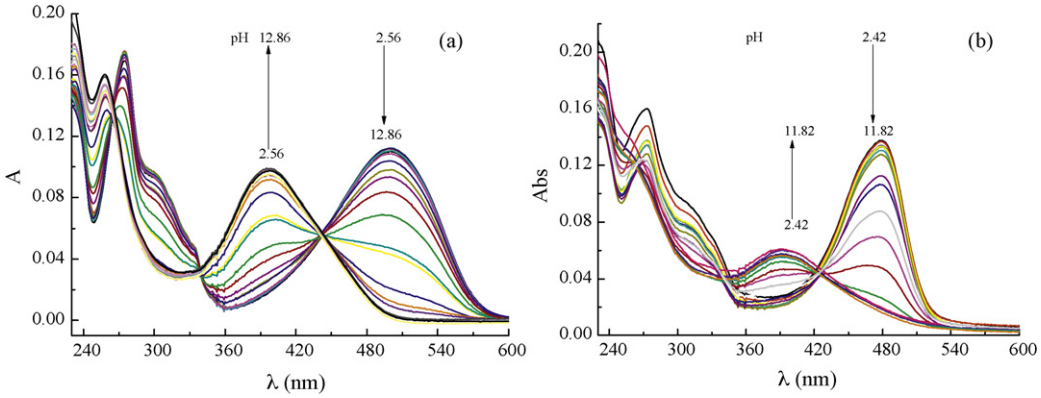

Fig. 1. pH effect on the UV–vis spectra of **6a** (a, [**6a**] = 6.5 μM) and **6b** (b, [**6b**] = 6.2 μM).

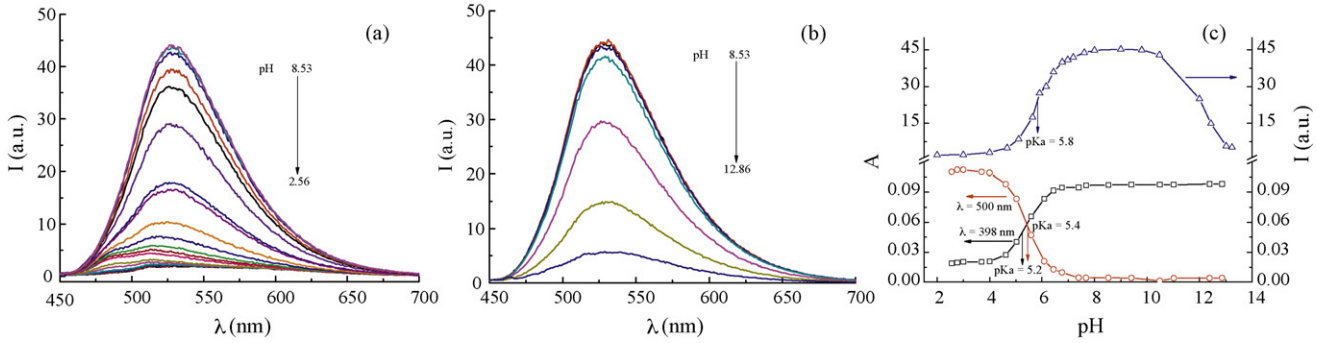

Fig. 2. pH effects on the emission spectra of **6a** (a and b); plots of fluorescence intensity and absorbance of **6a** vs. pH (c, excited at 445 nm) (blue line represents the change of fluorescence intensity; black and red lines represent the changes of absorbance at 398 and 500 nm, respectively. pK_a values were obtained according to Eqs. (1) and (2). (For interpretation of the references to color in the figure legend, the reader is referred to the web version of the article.)

For another isomer **6b**, when pH changes from 2.0 to 12.0, the absorbance at 478 nm was decreased significantly with an ~85 nm blue-shift in absorption maximum and an isosbestic point at 424 nm was clearly seen (Fig. 1b).

Although **6a** and **6b** are weak fluorescent in aqueous solution due to their TICT state, pH also affects their emission spectra significantly. As shown in Fig. 2, the fluorescence intensity of **6a** in aqueous solution is significantly quenched in 526 nm upon addition of aqueous hydrochloric acid (from pH 8.53 to 2.56, Fig. 2a), and a very weak red-shift emission (λ_{max} = 543 nm) is observed. The addition of NaOH (from pH 8.53 to 12.86, Fig. 2b) also led to a decrease in fluorescence intensity, and an "off–on–off" fluorescence response towards pH is achieved (Fig. 2c, blue line).

pH affects the fluorescence spectrum of **6b** in another way. The emission spectra of **6b** had no obvious change with the addition of HCl aqueous solution. While, the titration of NaOH induced large decrease in fluorescence intensity until the fluorescence was almost fully quenched (Fig. 3a). The λ_{em} value of **6b** shifted about 55 nm to red region in basic solution, which may be caused by the dimerization of **6b** [44,45].

From Figs. 2c and 3b, it can be seen that regioisomers **6a** and **6b** show very different pH dependent fluorescence properties. For **6a**, the emission is switched "off" at pH < 4 and pH > 13, and the fluorescence intensity is almost unchanged in pH range of 8–11. The dynamic detection windows are 4.5–7.0 and 10.5–13.0 in acidic/neutral and neutral/alkaline pH ranges, respectively; the

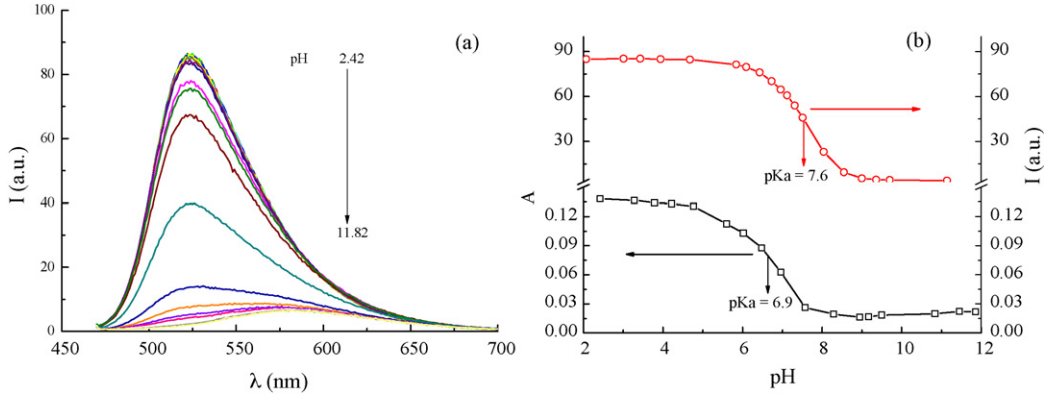

Fig. 3. pH effects on the emission spectra of **6b** (a); plots of fluorescence intensity (red line) and absorbance (black line) vs. pH of **6b** (b, excited at 424 nm; pK_a values were obtained according to Eqs. (1) and (2). (For interpretation of the references to color in the figure legend, the reader is referred to the web version of the article.)

Table 1
Spectra data and pK_a values of sensors.

Sensor	λ_{abs} (nm)	log ε	λ_{em} (nm)	Φ_F	pK_a (abs)	pK_a (fl)
6a	398[a]/500[b]	4.16[a]/4.25[b]	526[a]/543[b]	0.009 [a] / 0.001 [b]	5.4	5.8
6b	393[a]/478[b]	3.96[a]/4.32[b]	581[a]/523[b]	0.001[a]/0.015[b]	6.9	7.6

Note: the data obtained from basic[a] and acidic[b] solutions, respectively.

former is in the physiological range. Importantly, taking advantage of the solution's color change, we can distinguish the two distinct pH ranges of **6a**: the acidic solution of **6a** is red, while its alkaline solution is yellow. In the case of **6b**, the emission is switched off at pH > 9.0 and switched on at pH < 6 and the fluorescent detection window is 6.0–8.5.

The different fluorescence responses of **6a** and **6b** towards pH may be related to different excited state forms of protonated **6a**/**6b**. It can be seen in Scheme 2 that there are two forms (**A** and **B**) of protonated **6a**/**6b**. In the case of form **A**, the protonated imine enhanced the stability of excited state by reducing the electron density and then the solvation of water. But for form **B**, the protonated compound induced another TICT excited state, i.e. rotation of amino group in five-membered ring, which further quenched the fluorescence. The change in the distribution of the electronic density before and after protonation of **6a**/**6b** (after protonation, the electron density of imide N in **6a** increased whereas that in **6b** decreased, which was obtained by Gauss 3.0 software, Aptech Systems, Inc.) suggested that protonated **6a** mainly existed as form **B**, while protonated **6b** mainly present as form **A**. As a result, the protonation of **6a** quenched the fluorescence while that of **6b** enhanced the fluorescence.

The pH dependence of absorbance and fluorescence intensity (Figs. 2c and 3b) can be analyzed with Eqs. ((1) and (2)) [50] to give pK_a values listed in Table 1.

$$\log\left[\frac{(A_{max}-A)}{(A-A_{min})}\right] = pH - pK_a \quad (1)$$

$$\log\left[\frac{(I_{F\,max}-I_F)}{(I_F-I_{F\,min})}\right] = pH - pK_a \quad (2)$$

Table 1 reveals that isomers **6a** and **6b** show distinct differences in their photophysical properties: (1) the molar absorption coefficient of **6a** is a little bit higher in acidic solution than in basic one, while that of **6b** is much larger in acidic solution; (2) the maxima of both emission and absorption spectra of **6a** shifts to the blue-edge in response to OH^-, but the addition of alkali to **6b** aqueous solution results in a blue-shift in absorption and a red-shift in emission, and an unusual large stokes shift (about 190 nm) of **6b** in basic solution is observed; (3) the pK_a of **6a** is about 1.5 pH units lower than that of **6b**, which shows that **6a** is more difficult to be protonated; these discrepancies may be caused by the geometry distinctions, which leads to different distribution of electron density [51]. Table 1 also shows that the pK_a values obtained by fluorescence are obviously higher than those obtained by UV spectra method. As twist intramolecular charge transfer (TICT) sensors, the charge separation is more complete in the lowest excited singlet state, which leads to larger dipole moments in excited state than in ground state, so, **6a** and **6b** are easier to be protonated in the excited state [52,53]. As a result, the pK_a values obtained by fluorescence are larger.

4.2. Solvent effects on the photophysical properties of *6a* and *6b*

Table 2 illustrates the spectral data of dyes **6a** and **6b** in different solvents. It can be seen that in CH_2Cl_2, ethyl acetate (AcOEt) and CH_3CN, **6a** and **6b** have moderate fluorescence quantum yields (Φ_F), but in MeOH and water, the Φ_F values are very small. The stokes shift increases with the increasing polarity of solvent except for **6b** in water. The TICT state is stabilized by the polar solvents [52,53], as a consequence, the conjugation is lost, the absorption bands shift to shorter wavelengths and the fluorescence is quenched by the internal rotation [54]. It is notable that the molar absorption coefficient of **6a** is a litter lower in water than in other solvents, but that of **6b** is a bit higher in water, the latter may be attributed to part protonation of **6b** in water (its pK_a = 6.9, while the pH of water is ~6.5).

4.3. Surfactant effects on the absorption and emission spectra of *6a* and *6b*

4.3.1. CTAB

Fig. 4 shows the CTAB effect on the absorption and emission spectra of **6a**. It can be seen that with increasing CTAB concentration, the absorption band centered at 400 nm increased with ~5 nm red-shift at the expense of the shoulder band at 485 nm, yielding an isosbestic point at 445 nm (Fig. 4a). At the same time, the fluorescence intensity was enhanced significantly with about 15 nm blue-shift.

In the case of **6b**, when CTAB concentration was increased from 0 to 3.6 mM, the original absorption band centered at 478 nm decreased monotonically without remarkable wavelength shift, while the fluorescence intensity increased slightly with ~5 nm red-shift (Fig. 5).

4.3.2. Triton X-100

Triton X-100 induced similar changes in the absorption and emission spectra of **6a** and **6b** (data shown in supporting information, Figs. S2–3).

4.3.3. SDS

In addition to the significant intensity changes in the absorbance, the titration of SDS to **6a** aqueous solution also induced remarkable wavelength shift in absorption (~90 nm red-shift) (Fig. 6). When SDS was increased from 0 to 5.15 mM, the original absorption band centered at 398 nm was decreased monotonically.

Table 2
Spectral data of **6a** and **6b** in different solvents.

Solvent		**6a**				**6b**			
	Dielectric constants	λ_A (nm)	log ε	λ_F (nm)	Φ_F	λ_A (nm)	log ε	λ_F (nm)	Φ_F
CH_2Cl_2	9.1	403	4.20	498	0.291	400	4.05	518	0.343
AcOEt	4.3	392	4.20	496	0.263	390	4.10	515	0.233
CH_3CN	36.6	399	4.22	511	0.120	395	4.21	535	0.237
MeOH	32.7	408	4.24	519	0.008	410	4.15	556	0.051
H_2O	78.5	398	4.16	526	0.002	478	4.20	523	0.006

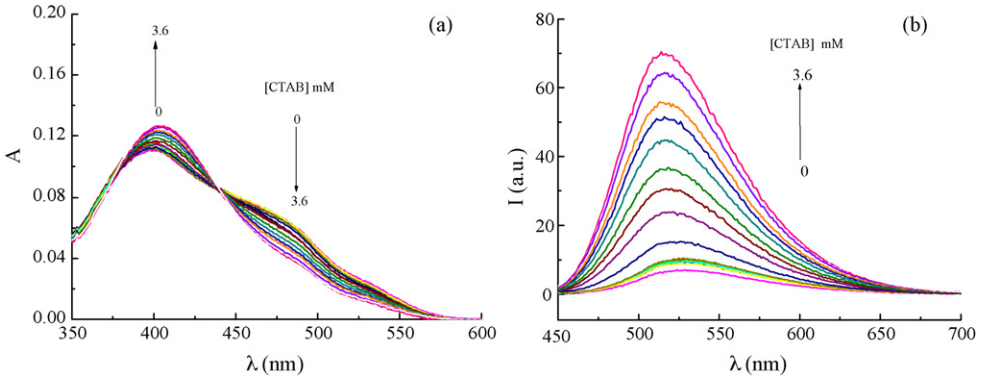

Fig. 4. CTAB effects on the absorption (a) and emission (b) spectra of **6a** (excited at 445 nm).

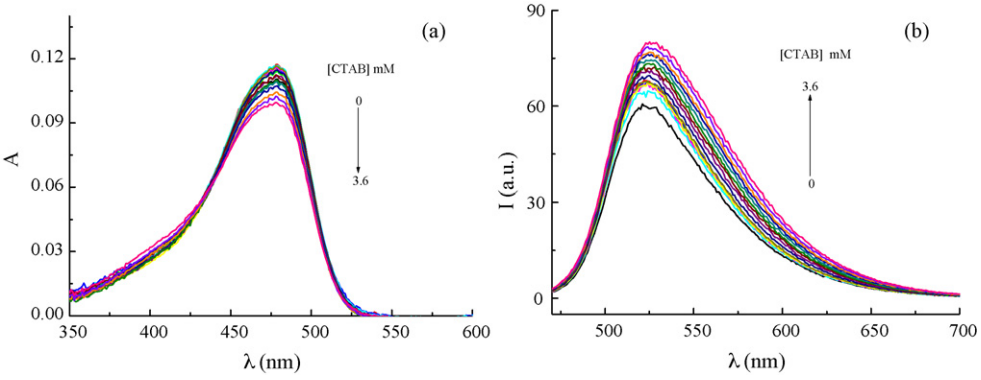

Fig. 5. CTAB effects on the absorption (a) and emission (b) spectra of **6b** (excited at 424 nm).

Beyond this, a new band centered at 485 nm was formed and developed, and the solution's color changed from yellow to orange red.

Fig. 7 presents the fluorescence spectral response towards SDS. When SDS concentration was increased from 0 to 5.15 mM, the emission band centered at 525 nm was slightly quenched without noticeable wavelength shift. Further addition of SDS (>6.06 mM) resulted in the recover of fluorescence with ~15 nm blue-shift in emission band.

For **6b**, when SDS concentration increased from 0 to 5.15 mM, the absorbance at 479 nm decreased monotonously from $\varepsilon = 1.57 \times 10^4$ to $0.73 \times 10^4\ M^{-1}\ cm^{-1}$ without notable wavelength shift. Above this, it increased steadily ($\varepsilon = 2.33 \times 10^4\ M^{-1}\ cm^{-1}$ at SDS = 12.72 mM, Fig. 8).

Similar trends in the emission spectra are also observed. The fluorescence intensity decreases with increasing [SDS] until it reaches the minimum at [SDS] = 6.06 mM, this change occurs in almost the same surfactant concentration region as the absorbance decreases. At [SDS] beyond 6.06 mM, the emission intensity increases with about 12 nm blue-shift of emission band compared to that in water (Fig. 9).

6a ($pK_a = 5.4$) is a nonionic compound, while **6b** ($pK_a = 6.9$) is tinily positively charged in neutral aqueous solution. So, no strong electrostatic interaction between **6a**/**6b** and surfactant was present. But **6a** and **6b** prefer hydrophobic environment due to two methyl groups with them, and the hydrophobic interaction between **6a**/**6b** and surfactants makes **6a**/**6b** be located in surfactant micelles. On

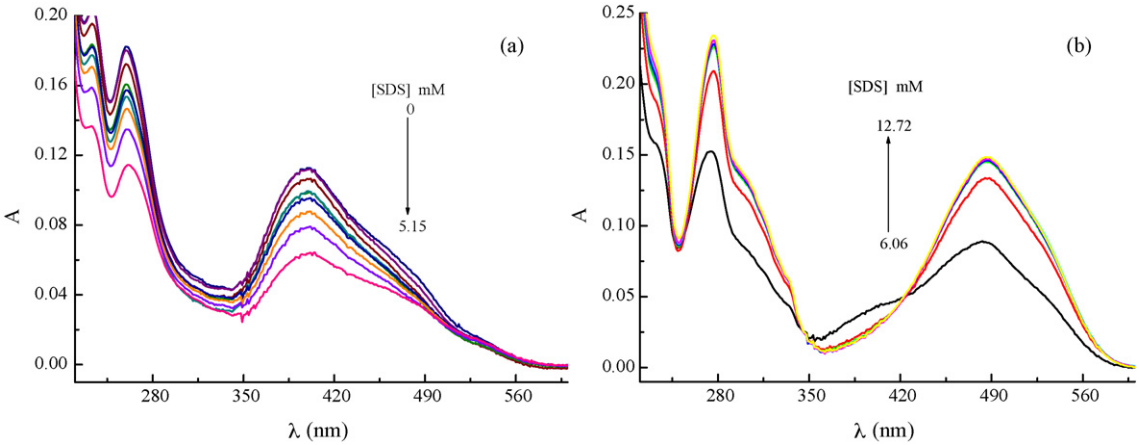

Fig. 6. SDS effects on the absorption spectra of **6a**.

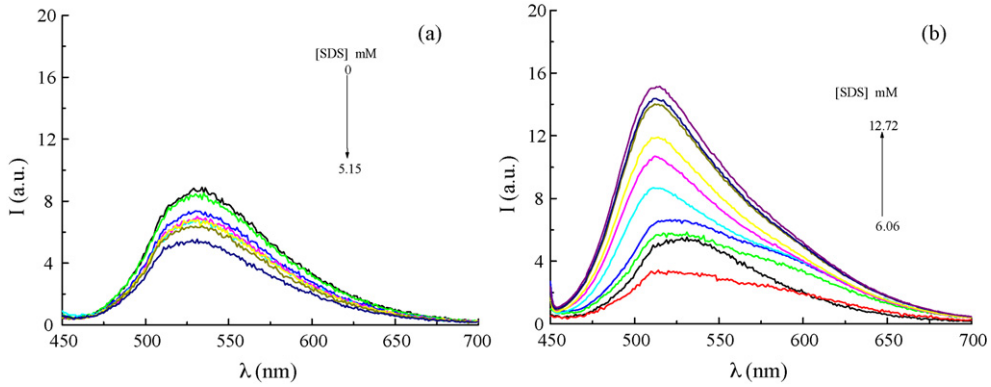

Fig. 7. SDS effects on the emission spectra of **6a** (excited at 445 nm).

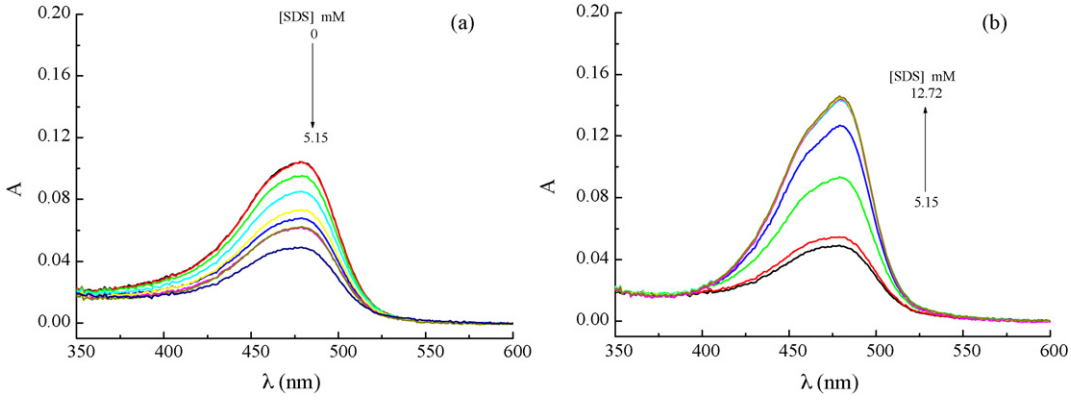

Fig. 8. SDS effects on the absorption spectra of **6b**.

one hand, micelles provide a less polar and more viscous microenvironment for dyes, which restricts the TICT state. As a consequence, the fluorescence intensity is enhanced accompanied with blue-shift in emission band. On the other hand, the amplifying effect on the local counterion concentration makes the change tendency of pH value vary with the surfactants' charge character. Therefore, the photophysical properties of **6a**/**6b** alter with the charge characters of surfactants. pH influences the spectral properties of **6a** and **6b** in different ways. In the case of **6a**, the absorbance at 500 nm decreases while that at 398 nm and the fluorescence intensity increase with increasing pH value. But for **6b**, when pH value is raised, both the absorbance and fluorescence intensity decrease.

Cationic surfactant CTAB can adsorb counterion OH^-, so the OH^- concentration is much higher around CTAB micelle than in bulk solution. The less polar and more viscous microenvironment along with higher OH^- concentration provided by CTAB micelle make the fluorescence intensity and absorbance at 398 nm of **6a** increase. The less polar CTAB micelles also cause the emission band shift to shorter wavelength (Fig. 4). The less polar microenvironment increases while the larger pH value decreases the fluorescence intensity of **6b**, but its absorbance at 478 nm decreases in both situations. As a result, the fluorescence intensity of **6b** increases slightly, but the absorbance decreases with the addition of CTAB. The slight red-shift in emission band (Fig. 5) is caused by the larger pH value around CTAB micelle.

The property of nonionic surfactant Triton X-100 is somewhat similar to that of cationic surfactant [55], so, Triton X-100 induces similar variation of the photophysical properties of **6a** and **6b**.

SDS affects the photophysical properties of **6a** and **6b** in a way different from that of CTAB. Both the absorbance and fluorescence

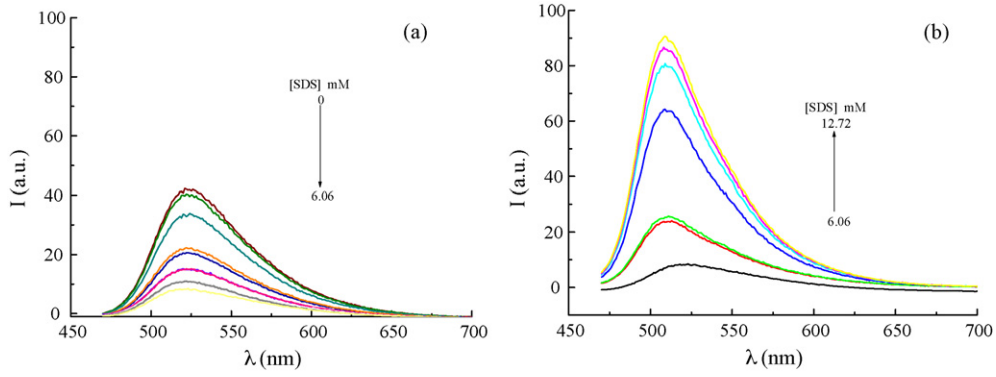

Fig. 9. SDS effects on the emission spectra of **6b** (excited at 424 nm).

Table 3
Truth table of **6a** in different conditions.

Input 1 H^+ (0.1 mM)	Input 2 OH^- (0.1 mM)	Output 1 A_{398}	Output 2 A_{500}	Output 3 I_F
0	0	0.112 (1)	0.040 (0)	9 (0)
0	1	0.136 (1)	0.012 (0)	45 (1)
1	0	0.003 (0)	0.145 (1)	4 (0)
1	1	0.124 (1)	0.035 (0)	12 (0)
		IMPLY	**INH**	**INH**

intensity decrease at SDS concentrations smaller than 6 mM (close to its cmc), and they increase above this concentration. The main difference between SDS and CTAB/Triton X-100 lies on their charge character of polar group.

Although the positive charge densities of **6a**/**6b** are relatively weak, **6a**/**6b** may form mixed aggregates with SDS (at [SDS] < cmc) like many cationic dyes [56–62] driven by the hydrophobic and coulomb interactions between them, which lead to the decreases of absorption and emission intensities at the maxima in the original spectra.

When SDS concentration is higher than 6 mM, SDS molecules begin to self-aggregate and form micelles. All dye molecules are incorporated into normal micelles in monomeric form. As a consequence, the microenvironmental polarity surrounding dye molecules is depressed, which leads to an enhancement in fluorescence intensity and a blue-shift of emission band. In addition, counter ion H^+ is adsorbed on the surface of SDS micelles, and the H^+ concentration is much higher at SDS micellar surface than in bulk solution, therefore, dye molecules are easier to be protonated with associated enhancement in the "push–pull" character of the ICT transition resulting in a red-shift (90 nm for **6a** and 3 nm for **6b**) in absorption spectrum accompanied with an increase in absorbance.

4.4. Molecular logic gates of two-input systems

When **6a** and **6b** were used as logic gates, they accomplished different logic functions due to their remarkably difference in photophysical properties. Compound **6a** has three output signals, when it is used to perform Boolean logic, more than one logic function will be achieved [11]. Table 3 shows that INHIBIT and IMPLICATION functions can be realized within **6a** with H^+ and OH^- as inputs along with A_{398}, A_{500} and I_F as outputs, respectively.

After understanding the properties of surfactants (e.g. form various aggregates related to their concentrations, local concentrated counter-ion, nanospace of micelles, etc.) and their effects on the spectral properties of **6a** and **6b**, we speculated that surfactants could provide a new strategy of advancing the field of molecular logic. So, we exploited surfactants for the design of supramolecular systems to realize molecular logic. The experimental results showed that surfactant not only increased the number of simple logic functions but also enabled complicated logic calculations to be performed at molecular level.

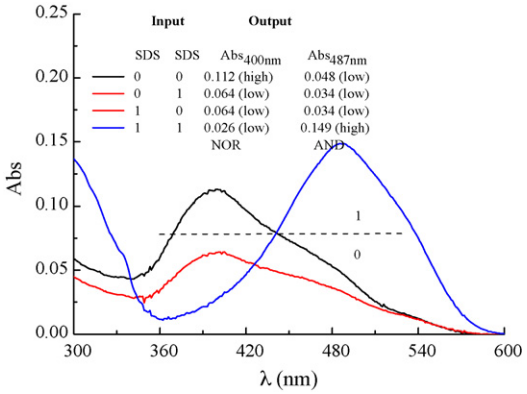

Fig. 10. Absorption and emission spectra and truth table of **6a** in water in the presence of chemical inputs.

Table 4
Truth table of **6a** in different conditions.

Input 1 SDS (10.4 mM)	Input 2 H^+ (10^{-4} M)	Output 1 A_{398}	Output 2 A_{500}
0	0	0.105 (1)	0.040 (0)
0	1	0.003 (0)	0.140 (1)
1	0	0.019 (0)	0.132 (1)
1	1	0.005 (0)	0.145 (1)
		NOR	**OR**

Herein, we demonstrate the logic functions completed within **6a** in SDS system. Fig. 10 shows the absorption spectra and the truth table of **6a** in different conditions, in which both two inputs are SDS with concentration being 0 (low) or 5.2 mM (high). The absorbance at 487 nm is high only in the case of both inputs kept high, so AND logic function is achieved in **6a** aqueous solution with output being the absorbance at 487 nm. The NOR logic function is realized in the same system with A_{400nm} as output.

When 10.4 mM SDS and 10^{-4} M OH^- are used as inputs, the IMPLICATION, INHIBIT and YES logic functions can be implemented with A_{400}, A_{478} and fluorescence intensity as outputs, respectively (Fig. 11). Whereas NOR and OR logic functions are achieved with the same outputs simply by using H^+ instead of OH^- (Table 4).

Compared with **6a**, **6b** can execute very different but much less logic functions (Tables S1–3). However, half addition can be accomplished with **6b**. Fig. 12 displays the absorption and emission spectra as well as the truth table of **6b** in different conditions, in which SDS concentration is 0 (low) or 5.2 mM (high). The fluorescence intensity (I_F) is high only in the case of both inputs kept high. The absorbance at 480 nm is high when two inputs are kept the

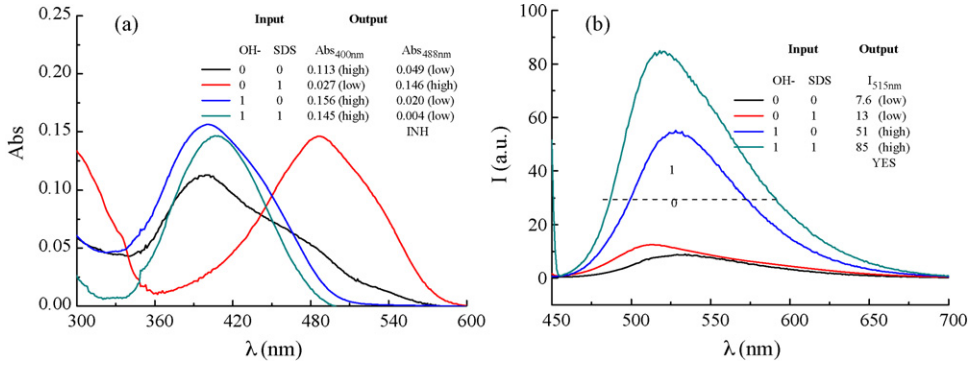

Fig. 11. Absorption and emission spectra and truth table of **6a** in water in the presence of chemical inputs.

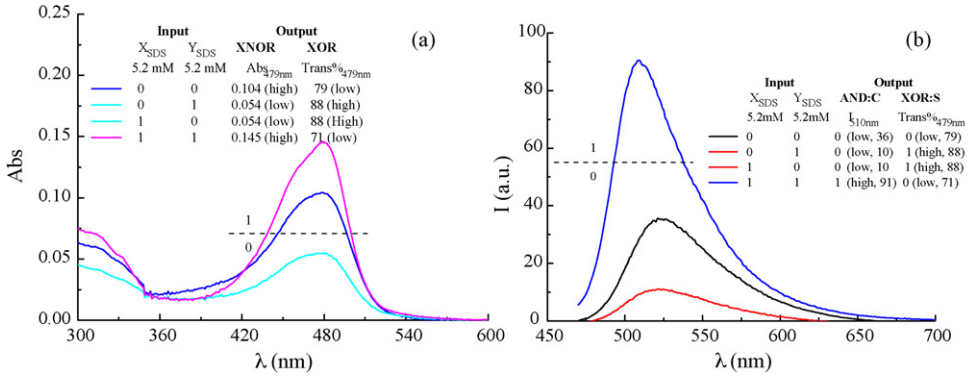

Fig. 12. Absorption and emission spectra as well as truth table of **6b** in water in the presence of chemical inputs.

same. So, AND and XNOR gates are obtained when the outputs are I_F and A_{478}, respectively. With the transmittance at 478 nm used as output, the XOR gate is achieved. Therefore, half addition is carried out when both inputs are SDS.

5. Conclusions

Isomeric compounds **6a** and **6b** are environment sensitive. Their spectral responses towards pH and environmental polarity are different. In addition to altering the properties of microenvironment where dyes located, anionic surfactant SDS can also form complexes with **6a** (or **6b**), which endows **6a** (or **6b**) with multiple spectral output signals and makes much more logic functions be completed with **6a** (or **6b**). Different from the results obtained in our previous work, cationic surfactant CTAB and nonionic surfactant Triton X-100 enhance the fluorescence intensities of **6a** and **6b** due to the less polarity, more viscosity and higher pH value of micelles. Resulting from the different distribution of electron density, isomers **6a** and **6b** perform different logic functions with the same inputs: **6a** can execute more logic functions, while **6b** can implement logic calculation.

Acknowledgements

This work was financially supported by the National Natural Science Foundation of China (20536010), the National Key Project for Basic Research (2003CB 114400) and the Science and Technology Foundation of Shanghai.

Appendix A. Supplementary data

Supplementary data associated with this article can be found, in the online version, at doi:10.1016/j.jphotochem.2009.07.006.

References

[1] A.P. de Silva, H.Q.N. Gunaratne, C.P. McCoy, A molecular photoionic AND gate based on fluorescent signaling, Nature 364 (1993) 42–44.
[2] A.P. de Silva, N.D. Mcclenaghan, Simultaneously multiply-configurable or superposed molecular logic systems composed of ICT (internal charge transfer) chromophores and fluorophores integrated with one- or two-ion receptors, Chem. Eur. J. 8 (2002) 4935–4945.
[3] A.P. de Silva, N.D. Mcclenaghan, Molecular-scale logic gates, Chem. Eur. J. 10 (2004) 574–586.
[4] Z. Wang, G. Zheng, P. Lu, 9-(Cycloheptatrienylidene)-fluorene derivative: remarkable ratiometric pH sensor and computing switch with NOR logic gate, Org. Lett. 7 (2005) 3669–3671.
[5] A.P. de Silva, S. Uchiyama, T.P. Vance, B. Wannalerse, A supramolecular chemistry basis for molecular logic and computation, Coord. Chem. Rev. 251 (2007) 1623–1632.
[6] D.C. Magri, T.P. Vance, A.P. de Silva, From complexation to computation: recent progress in molecular logic, Inorg. Chim. Acta 360 (2007) 751–764.
[7] Z. Zhao, Y. Xing, Z. Wang, P. Lu, Dual-fluorescent donor–acceptor dyad with tercarbazole donor and switchable imide acceptor: promising structure for an integrated logic gate, Org. Lett. 9 (2007) 547–550.
[8] D.C. Magri, G.D. Coen, R.L. Boyd, A.P. de Silva, Consolidating molecular AND logic with two chemical inputs, Anal. Chim. Acta 568 (2006) 156–160.
[9] A.P. de Silva, H.Q.N. Gunaratne, C. McCoy, Molecular photoionic AND logic gates with bright fluorescence and "Off–On" digital action, J. Am. Chem. Soc. 119 (1997) 7891–7892.
[10] A. Credi, V. Balzani, S.J. Langford, J.F. Stoddart, Logic operations at the molecular level. An XOR gate based on a molecular machine, J. Am. Chem. Soc. 119 (1997) 2679–2681.
[11] H.T. Baytekin, E.U. Akkaya, A molecular NAND gate based on Watson–Crick base pairing, Org. Lett. 2 (2000) 1725–1727.
[12] J. Mataui, M. Mitsuishi, A. Aoki, T. Miyashita, Optical logic operation based on polymer Langmuir–Blodgett-film assembly, Angew. Chem. Int. Ed. 42 (2003) 2272–2275.
[13] G. Zhang, D. Zhang, Y. Zhou, D. Zhu, A new tetrathiafulvalene–anthracence dyad fusion with the crown ether group: fluorescence modulation with Na^+ and C_{60}, mimicking the performance of an "AND" logic gate, J. Org. Chem. 71 (2006) 3970–3972.
[14] M.N. Stojanovic, D. Stefanovic, Deoxyribozyme-based half-adder, J. Am. Chem. Soc. 125 (2003) 6673–6676.
[15] S.J. Langford, T. Yann, Molecular logic: a half-subtractor based on tetraphenylporphyrin, J. Am. Chem. Soc. 125 (2003) 11198–11199.
[16] A. Okamoto, K. Tanaka, I. Saiti, DNA logic gates, J. Am. Chem. Soc. 126 (2004) 9458–9463.
[17] D. Margulies, G. Melman, C.E. Felder, R. Arad-Yellin, A. Shanzer, Chemical input multiplicity facilitates arithmetical processing, J. Am. Chem. Soc. 126 (2004) 15400–15401.
[18] X. Guo, D. Zhang, G. Zhang, D. Zhu, Monomolecular logic: "half-adder" based on multistate/multifunctional photochromic spiropyrans, J. Phys. Chem. B 108 (2004) 11942–11945.
[19] D. Margulies, G. Melman, A. Shanzer, Fluorescein as a model molecular calculator with reset capability, Nature Mater. 4 (2005) 768–771.
[20] D. Qu, Q. Wang, H. Tian, A half adder based on a photochemically driven [2]rotaxane, Angew. Chem. Int. Ed. 44 (2005) 5296–5299.
[21] A. Coskun, E. Deniz, E.U. Akkaya, Effective PET and ICT switching of boradiazaindacene emission: a unimolecular, emission-mode, molecular half-subtractor with reconfigurable logic gates, Org. Lett. 7 (2005) 5187–5189.
[22] D. Margulies, G. Melman, A. Shanzer, A molecular full-adder and full-subtractor, an additional step toward a moleculator, J. Am. Chem. Soc. 128 (2006) 4865–4871.
[23] R. Baron, O. Lioubashevski, E. Katz, T. Niazov, I. Willner, Elementary arithmetic operations by enzymes: a model for metabolic pathway based computing, Angew. Chem. Int. Ed. 45 (2006) 1572–1576.
[24] Y. Zhou, H. Wu, L. Qu, D. Zhang, D. Zhu, A new redox-resettable molecule-based half-adder with tetrathiafulvalene, J. Phys. Chem. B 110 (2006) 15676–15679.
[25] H.-F. Ji, R. Dabestani, G.M. Brown, A supramolecular fluorescent probe, activated by protons to detect cesium and potassium ions, mimics the function of a logic gate, J. Am. Chem. Soc. 122 (2000) 9306–9307.
[26] A. Saghatelian, N.H. Völcker, K.M. Guckian, V.S.-Y. Lin, M.R. Ghadiri, DNA-based photonic logic gates: AND, NAND, and INHIBIT, J. Am. Chem. Soc. 125 (2003) 346–347.
[27] Y. Shiraishi, Y. Tokitoh, T. Hirai, A fluorescent molecular logic gate with multiply-configurable dual outputs, Chem. Commun. (2005) 5316–5318.
[28] K. Szacilowski, W. Macyk, G. Stochel, Light-driven OR and XOR programmable chemical logic gates, J. Am. Chem. Soc. 128 (2006) 4550–4551.
[29] B.M. Frezza, S.L. Cockroft, M.R. Ghadiri, Modular multi-level circuits from immobilized DNA-based logic gates, J. Am. Chem. Soc. 129 (2007) 14875–14879.
[30] K. Rurack, C. Trieflinger, A. Koval'chuck, J. Daub, An ionically driven molecular IMPLICATION gate operating in fluorescence mode, Chem. Eur. J. 13 (2007) 8998–9003.

[31] D.M. Vriezema, M.C. Aragonès, J.A.A.W. Elemans, J.J.L.M. Cornelissen, A.E. Rowan, R.J.M. Nolte, Self-assembled nanoreactors, Chem. Rev. 105 (2005) 1445–1490.
[32] Y. Wan, H. Yang, D. Zhao, Host–guest" chemistry in the synthesis of ordered nonsiliceous mesoporous materials, Acc. Chem. Res. 39 (2006) 423–432.
[33] K. Niikura, E.V. Anslyn, Triton X-100 enhances ion-pair-driven molecular recognition in aqueous media. Further work on a chemosensor for inositol trisphosphate, J. Org. Chem. 68 (2003) 10156–10157.
[34] A. Mallick, M.C. Mandal, B. Haldar, A. Chakrabarty, P. Das, N. Chattopadhyay, Surfactant-induced modulation of fluorosensor activity: a simple way to maximize the sensor efficiency, J. Am. Chem. Soc. 128 (2006) 3126–3127.
[35] Y. Zhao, Z. Zhong, Detection of Hg^{2+} in aqueous solutions with a foldamer-based fluorescent sensor modulated by surfactant micelles, Org. Lett. 8 (2006) 4715–4717.
[36] Y. Diaz-Fernandez, F. Foti, C. Mangano, P. Pallavicini, S. Patroni, A. Perez-Gramatges, S. Rodriguez-Calvo, Micelles for the self-assembly of "Off–On–Off" fluorescent sensors for pH windows, Chem. Eur. J. 12 (2006) 921–930.
[37] J. Wang, X. Qian, J. Qian, Y. Xu, Micelle-induced versatile performance of amphiphilic intramolecular charge-transfer fluorescent molecular sensors, Chem. Eur. J. 13 (2007) 7543–7552.
[38] A.A. Agbodjan, H. Bui, M.G. Khaledi, Study of solute partitioning in biomembrane–mimetic pseudophases by electrokinetic chromatography: dihexadecyl phosphate small unilamellar vesicles, Langmuir 17 (2001) 2893–2899.
[39] G. von Maltzahn, S. Vauthey, S. Santoso, S. Zhang, Positively charged surfactant-like peptides self-assemble into nanostructures, Langmuir 19 (2003) 4332–4337.
[40] X. Huang, Z. Dong, J. Liu, S. Mao, J. Xu, G. Luo, J. Shen, Selenium-mediated micellar catalyst: an efficient enzyme model for glutathione peroxidase-like catalysis, Langmuir 23 (2007) 1518–1522.
[41] A. Roque, F. Pina, S. Alves, R. Ballardini, M. Maestri, V. Balzani, Micelle effect on the "write–lock–read–unlock–erase" cycle of 4′-hydroxyflavylium ion, J. Mater. Chem. 9 (1999) 2265–2269.
[42] S. Uchiyama, G.D. McClean, K. Iwai, A.P. de Silva, Membrane media create small nanospaces for molecular computation, J. Am. Chem. Soc. 127 (2005) 8920–8921.
[43] H. Zhang, X. Lin, Y. Yan, L. Wu, Luminescent logic function of a surfactant-encapsulated polyoxometalate complex, Chem. Commun. (2006) 4575–4577.
[44] J. Qain, X. Qian, Y. Xu, S. Zhang, Multiple molecular logic functions and molecular calculations facilitated by surfactant's versatility, Chem. Commun. (2008) 4141–4143.
[45] J. Qian, Y. Xu, X. Qian, S. Zhang, Molecular logic operations based on surfactant nanoaggregates, ChemPhysChem 9 (2008) 1891–1898.
[46] Z. Diwu, C.-S. Chen, C. Zhang, D.H. Klaubert, R.P. Haugland, A novel acidotropic pH indicator and its potential application in labeling acidic organelles of live cells, Chem. Biol. 6 (1999) 411–418.
[47] S. Charier, O. Ruel, J.-B. Baudin, D. Alcor, J.-F. Allemand, A. Meglio, L. Jullien, An efficient fluorescent probe for ratiometric pH measurements in aqueous solutions, Angew. Chem. Int. Ed. 43 (2004) 4785–4788.
[48] H. Ihmels, A. Meiswinkel, C.J. Mohrschladt, D. Otto, M. Waidelich, M. Towler, R. White, M. Albrecht, A. Schnurpfeil, Anthryl-substituted heterocycles as acid-sensitive fluorescence probes, J. Org. Chem. 70 (2005) 3929–3938.
[49] J.F. Callan, A.P. de Silva, J. Ferguson, A.J.M. Huxley, A.M. O'Brien, Fluorescent photoionic devices with two receptors and two switching mechanisms: applications to pH sensors and implications for metal ion detection, Tetrahedron 60 (2004) 11125–11131.
[50] A.P. de Silva, H.Q.N. Gunaratne, P.L.M. Lynch, A.J. Patty, G.L. Spence, Luminescence and charge transfer. Part 3. The use of chromophores with ICT (internal charge transfer) excited states in the construction of fluorescent PET (photoinduced electron transfer) pH sensors and related absorption pH sensors with aminoalkyl side chains, J. Chem. Soc. Perkin Trans. 2 (1993) 1611–1616.
[51] Y. Zhou, Y. Xiao, S. Chi, X. Qian, Isomeric boron–fluorine complexes with donor–acceptor architecture: strong solid/liquid fluorescence and large stokes shift, Org. Lett. 10 (2008) 633–636.
[52] B. Valeur, Molecular Fluorescence: Principles and Applications, Wiley-VCH Verlag GmbH, Weinheim, 2002.
[53] Y. Xiao, Doctoral Dissertation, Dalian University of Technology, Dalian, 2002.
[54] The absorption and emission wavelengths of **6a** and **6b** are shorter than their analogs.
[55] G. Zhao, B. Zhu, Principles of Surfactant Action, Light Industry Press of China, Beijing, 2003.
[56] P. Mukerjee, K.J. Mysels, J. Am. Chem. Soc. 77 (1955) 2937.
[57] H. Sato, M. Kawasaki, K. Kasatani, Fluorescence and energy transfer of dyedetergent system in the premicellar region, J. Photochem. 17 (1981) 243–248.
[58] A. Yamagishi, F. Watanabe, Effects of an aliphatic tail on the interactions of an ionic dye and a polyelectrolyte. The system of N-alkylated acridine orange derivatives and poly(styrenesulfonic acid), J. Phys. Chem. 85 (1981) 2129–2134.
[59] P. Bilski, R.N. Holt, C.F. Chignell, Premicellar aggregates of Rose Bengal with cationic and zwitterionic surfactants, J. Photochem. Photobiol. A 110 (1997) 67–74.
[60] S. Biswas, S.C. Bhattacharya, P.K. Sen, S.P. Moulik, Absorption and emission spectroscopic studies of fluorescein dye in alkanol, micellar and microemulsion media, J. Photochem. Photobiol. A 123 (1999) 121–128.
[61] R.V. Pereira, M.H. Gehlen, Fluorescence of acridinic dyes in anionic surfactant solution, Spectrochim. Acta A 61 (2005) 2926–2932.
[62] T.A. Fayed, S.E.-D.H. Etaiw, N.Z. Saleh, Micellar effects on the molecular aggregation and fluorescence properties of benzazole-derived push–pull butadienes, J. Lumin. 121 (2006) 431–440.